Nature Environment and Pollution Technology
An International Quarterly Scientific Journal

p-ISSN: 0972-6268
(Print copies up to 2016)
e-ISSN: 2395-3454

Vol. 22 | No. 2 | pp. 639-652 | 2023

Original Research Paper

https://doi.org/10.46488/NEPT.2023.v22i02.008

Open Access Journal

# Removal of $H_2S$ from Biogas Using *Thiobacillus* sp.: Batch and Continuous Studies

**R. Shet and S. Mutnuri†**
Applied Environmental Biotechnology Laboratory, BITS Pilani, K.K. Birla Goa Campus, Zuarinagar, Goa-403726, India
†Corresponding author: S. Mutnuri; srikanth@goa.bits-pilani.ac.in

**Nat. Env. & Poll. Tech.**
**Website: www.neptjournal.com**

*Received:* 10-10-2022
*Revised:* 06-12-2022
*Accepted:* 22-12-2022

**Key Words:**
*Thiobacillus* sp.
$H_2S$ removal
Anaerobic co-digestion
Adsorption kinetics
Adsorption isotherms

## ABSTRACT

Anaerobic digestion produces biogas which usually contains 60-70% of methane ($CH_4$), 30-40% of carbon-di-oxide ($CO_2$), and 10-2,000 ppm hydrogen sulfide ($H_2S$). The concentration of $H_2S$ depends upon the type of substrate. $H_2S$ tends to corrode pipes and machines carrying them. The high concentrations of $H_2S$ present in biogas may adversely affect electricity generation. Hence, the removal of $H_2S$ and enrichment of biogas with $CH_4$ is an essential step towards higher energy production. In the present study, the biological method of removing $H_2S$ using *Thiobacillus* sp. was demonstrated for a one cu.m anaerobic co-digestion (ACD) unit running on an organic fraction of municipal solid waste (OFMSW) and septage sludge. Initial lab scale studies were conducted by collecting the biogas generated from 1 cu.m digesters, and continuous experiments were optimized for the process parameters such as flow rate, the volume of medium with culture, time, the height of the column, column composition, etc. The raw biogas was purged in a liquid medium (LM) with a culture containing *Thiobacillus* sp. The studies with the LM containing *Thiobacillus* sp. culture showed a 68% removal of $H_2S$ in the first 8 min, and the saturation occurred at 75 min when the time-dependent experiment was studied. The smaller flow rate (0.48 $L.min^{-1}$) and highest volume of culture (500 mL) showed better results than other parameters. The highest and average oxidation rates of sulfate were recorded as 39 and 40.3 $ppm.sec^{-1}$, respectively, for 0.48 $L.min^{-1}$ flow rate and 500 mL of the culture volume. In the column studies, a column containing cocopeat (CP) was studied for its efficiency in removing $H_2S$. At a flow rate of 0.9 $L.min^{-1}$, 25% adsorption was encountered and reached saturation at 90 min. The bed height of 9 inches with CP and plastic support (PS) showed a 20% $H_2S$ removal. The filling ratio of CP and PS (1:1) was the best ratio for proper gas passage with optimal time for adsorption/absorption. The kinetic, isotherm, and continuous models helped to understand the capacity of the adsorbent. Freundlich, Yoon-Nelson, and BDST model were best fit for the present study. A pilot scale setup for one cu.m biogas reactor showed an average of 50% removal of $H_2S$ for LM with culture, and an additional 20% removal was possible by the introduction of a column along with the liquid bed in series. An overall efficiency of 70-75% of $H_2S$ removal was achieved. No significant $CH_4$ loss was encountered during the study.

## INTRODUCTION

The anaerobic reduction of sulfur by the sulfur-reducing bacteria in the presence of hydrogen produced during the hydrolysis and fermentation process produces hydrogen sulfide ($H_2S$) gas. Sulfurs are present in organic compounds such as amino acids, enzymes, proteins, fats, etc. inorganic sulfur does not functionally interfere with any biological pathways; instead, it serves as a precursor for the synthesis of organic compounds (Jensen & Webb 1995). The biogas contains concentrations of $H_2S$ varying between 500 ppm to 20,000 ppm depending on the type and nature of substrates (Pokorna & Zabranska 2015). The biogas generated from different substrates contains different concentrations of $H_2S$. For example, the biogas from organic waste contains 10-2,000 ppm of $H_2S$, and with sewage sludge as the substrate, it varies from 10-20,000 ppm of $H_2S$ respectively (Aslam et al. 2019, Dumont 2015, Monteleone et al. 2011).

Inhaling high concentrations of $H_2S$ can adversely affect humans, causing severe toxic sensory problems (Díaz et al. 2011). It is also harmful to cement and steel structures, such as old heritage monuments, where they can deteriorate the binding capacity of the cement and can accelerate rusting (de Oliveira et al. 2019). The biogas plants handling high amounts of liquids and gases containing $H_2S$ also affect the

steel structures like pipes and pumps, causing corrosion (Zhang et al. 2008). The flaring/burning of the biogas containing high $H_2S$ will lead to higher emissions of $SO_x$ into the environment. $H_2S$ is an airborne pollutant causing acute and chronic health problems depending on the exposure time and toxicant concentration (Aslam et al. 2019). Hence, it is important to remove the $H_2S$ content before utilizing the biogas without hampering the process of anaerobic co-digestion (ACD).

Different removal methods are available, applied, and studied over time, including physical such as scrubbing through water, carbon, etc. Moreover, chemical methods include adding NaOH (Bagreev et al. 2000) and using iron filling (Andriani et al. 2020, Ho et al. 2013) to oxidize $H_2S$. However, these methods are reliant on resources that are either expensive or require frequent regeneration. Micro aeration is another process of reducing $H_2S$ in biogas where limited oxygen will be supplied to the reactors at the outlet to oxidize the $H_2S$. However these method is extremely sensitive and may result in decreased reactor efficiency if not monitored (Pokorna & Zabranska 2015).

Several studies have explored the application of biological methods of $H_2S$ removal. *Thiobacillus* is one such species of microorganism that has the potential to oxidize sulfur compounds. Other organisms include *Acidophile, AcidiThiobacillus, Thiooxidans, Thiobacillus, Thioparus,* and *Pseudomonas* (Ramírez-Aldaba et al. 2016, Zicari 2003). These microbes have the potential to withstand high concentrations of $H_2S$, and they do not diminish quickly and can be sustained for a longer span of time (Lin et al. 2013). The use of *Thiobacillus* sp. to enrich biogas evokes a redox reaction, producing elemental sulfur (Zhao et al. 2010).

Adsorption is another method that can be implemented to remove $H_2S$. Many studies have been conducted to investigate column behavior toward adsorption. Different compounds have been used for the adsorption study, including activated carbon (de Oliveira et al. 2019), zeolites, and AD fibers (Ayiania et al. 2019, Kulkarni & Ghanegaonkar 2019, Shah et al. 2017), oil fly ash (Aslam et al. 2019), biochar (Sethupathi et al. 2017), cow manure compost (Zicari 2003), sugarcane bagasse (Pantoja et al. 2010) and use of molecular sieves (Georgiadis et al. 2021). Few studies have used cocopeat (CP) as an adsorbent to remove $H_2S$ (De Silvaa et al. 2019, Pantoja et al. 2010). Only a few studies have been reported using column and microbial culture broth (Dumont 2015). Kumari & Dey (2019) used CP as an adsorbent to remove malachite green dye from wastewater.

The present study aimed to remove $H_2S$ from the biogas obtained from ACD of OFMSW and septage using reactors containing liquid medium (LM) with *Thiobacillus* culture. The study aims to use a continuous column containing CP, plastic support (PS), and culture for $H_2S$ removal. Further, both these approaches were combined, and the combination of the two systems in series was implemented at 1 cu.m reactor ACD reactors to study the $H_2S$ removal efficiency.

## MATERIALS AND METHODS

### Primary Requirements

The raw biogas required for this study was collected from the existing 1 cu.m biogas digesters (R1 and R2). The Thiobacillus culture was prepared by dissolving the salts listed and represented in Table 1 using sterile distilled water (Pokorna & Zabranska 2015). The primary culture was prepared using 5% (v/v) domestic wastewater/sewage as inoculum, and it was subcultured to obtain concentrated *Thiobacillus* sp. culture. The inoculated media was incubated for nine days at room temperature under anaerobic conditions. The media showed a white, turbid, and denser texture as the incubation period passes, indicating *Thiobacillus* sp. proliferation. This culture was used for liquid bed (LM) studies and column experiments. The CP and PS for the column experiments were procured from the local vendors used as the adsorbent medium. The composition of biogas was analysed using Geotech BIOGAS 5000 portable biogas analyser.

### Liquid Bed Experiments

The raw biogas from digesters R1 and R2 were stored in 1.5 $m^3$ capacity biogas balloons. The liquid bed experiments began with purging raw biogas (mixture of $CH_4$, $CO_2$, and $H_2S$) into borosilicate bottles (500 mL capacity) containing LM with culture through the inlet port (Zhu et al. 2020). The outlet port was connected to a portable biogas analyzer, and the $CO_2$, $H_2S$, and $CH_4$ concentrations were measured at different intervals. The effect of different parameters such as flow rate, time, and amount of LM with culture on absorption was studied individually, keeping other parameters constant. The initial and final methane concentration ($CH_4$) through

Table 1: Chemical composition of the *Thiobacillus* sp. specific broth.

| Chemical salts | Quantity [$g.L^{-1}$] |
|---|---|
| Ammonium sulfate | 0.4 |
| Mono-potassium phosphate | 4 |
| Calcium chloride | 0.25 |
| Ferrous sulfate | 0.1 |
| Magnesium sulfate | 0.5 |
| Sodium thiosulfate | 5 |
| Agar | 20 |

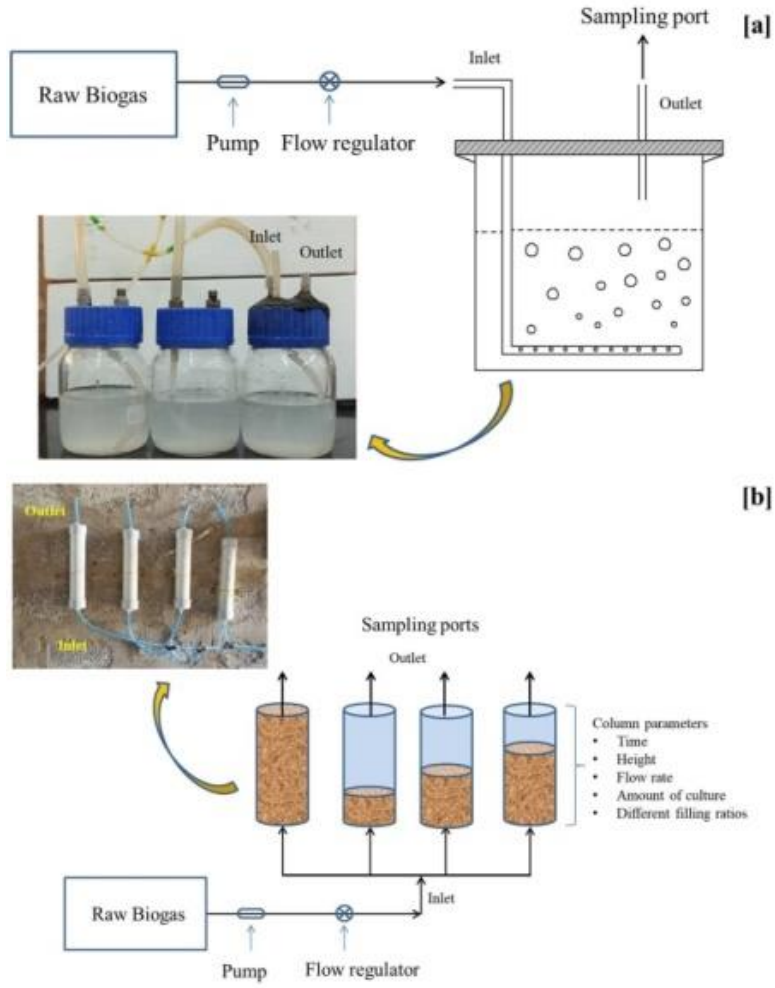


Fig. 1: $H_2S$ removal set up [a] liquid bed and [b] continuous column experiment.

LM with culture was recorded at varying times (0, 5, 10, 15, 20-200 min). Different flow rates of biogas, such as 0.48, 0.66, and 1.2 L.min$^{-1,}$ and amounts of culture as 100, 200, and 500 mL, were selected. Fig. 1[a] represents the setup and the real-time picture of the liquid bed filled with the culture.

**Continuous Column Experiments: Microorganism Cultivation and Immobilization**

The continuous column experiments were set up using PVC pipes (diameter 5.03 cm). For this study, different column parameters such as time, the height of the bed (3, 6, and 9 inches), amount of culture (0, 20, and 50 mL), the flow rate of the biogas (0.48, 0.66, and 1.2 mL.min$^{-1}$) and filling ratios of PS and CP (100% PS, 50:50 PS: CP and 20:80 PS: CP) were selected. The column was filled with different ratios of PS and CP, and the raw biogas was passed from the bottom using a 0.15 HP pump. The CP as a packing material offered a higher surface area for adsorption and microbes to proliferate.

To promote a uniform gas distribution through the column, the porosity of the packing material is crucial. The packing material should also have water absorption capacity so microorganisms can grow onto them (Fischer 2010). While a particular parameter was varied and studied, other parameters were kept constant for each experiment. The outlet was provided at the top, where biogas compositions were monitored using a portable biogas meter. Different flow rates were fixed using a gas flow meter at room temperature. The columns were provided with a headspace of 3 inches. The experiments were conducted until the saturation points were reached. The breakthrough curves were plotted between normalized concentration (C/Co) and time (Aslam et al. 2019, Ayiania et al. 2019). The breakthrough curve gives an understanding of the system's capacity to adsorb the particular gaseous component, in this case, the adsorption

Table 2: Mathematical forms of the kinetics and its parameters (Kumari & Dey 2019, Zulkefli et al. 2017).

| Models | Equation | Parameters |
|---|---|---|
| Adsorption kinetics | | |
| Pseudo first order | $\ln(qe - qt) = \ln qe = K1t$ | qe = adsorption capacity at equilibrium (mL.g$^{-1}$) |
| | | qt = adsorption capacity at time t (mL.g$^{-1}$) |
| | | $K_1$ = equilibrium constant for pseudo-first-order (min$^{-1}$) |
| | | t = time (min) |
| Pseudo second order | $\frac{t}{qt} = \frac{1}{K2\ qe^2} + \frac{t}{qt}$ | $K_2$ = equilibrium constant for pseudo-second-order (min$^{-1}$) |
| Elovich model | $qt = \frac{1}{\beta}\ln(\alpha\beta) + \frac{1}{\beta}\ln t$ | β = fraction of surface coverage (g.mL$^{-1}$) |
| | | α = initial adsorption rate (mL.(g.min$^{-1}$)) |
| Adsorption isotherms | | |
| Langmuir isotherm | $\frac{Ce}{q_m} = \frac{1}{q_m b} + \frac{Ce}{q_m}$ | Ce = concentration at equilibrium (ppm) |
| | | qm = maximum adsorption capacity (mg.mL$^{-1}$) |
| | | b = Langmuir constant (L.mg$^{-1}$) |
| Freundlich isotherm | $\log q_e = \log k_f + \frac{1}{n}\log Ce$ | kf = adsorption capacity parameter (mg.mL$^{-1}$) |
| | | n = Freundlich index |
| Continuous column study models | | |
| Thomas model | $\ln\frac{Co}{Ce} - 1 = \frac{kth\ qmax\ M}{Q} - kth\ Co\ t$ | Co = inlet concentration |
| | | Ce = outlet concentration |
| | | kth = Thomas constant (L.mg$^{-1}$.h$^{-1}$) |
| | | M = mass of adsorbent (g) |
| | | t = time (h) |
| Yoon–Nelson model | $ln\frac{Ce}{Co} = kYN\ t - J\ kYN$ | kYN = rate constant (min$^{-1}$) |
| | | J = time required for 50% adsorbate breakthrough (min) |
| Adams–Bohart model | $ln\frac{Ce}{Co} = kAB\ Co\ t - kAB\ No(\frac{Z}{Uo})$ | kAB = kinetic constant (L.mg$^{-1}$.min$^{-1}$) |
| | | No = saturation concentration (mL.kg$^{-1}$) |
| | | Z = bed depth of the fixed-bed column (cm) |
| | | Uo = superficial velocity (cm.min$^{-1}$) |

capacity of $H_2S$. The breakthrough point, which shows the adsorbent's maximum capacity, is responsible for knowing the highest bed volume (BV) (Sunzini et al. 2020, Zulkefli et al. 2017).

Fig. 1[b] shows the liquid bed and column experiment setups. To understand the column behavior of the adsorbent, several models such as BDST, Thomas model, Yoon-Nelson model, and Adams–Bohart model were studied and are expressed in the mathematical forms in Table 2.

## Performance of Optimized Condition for $H_2S$ Scrubbing at Pilot Scale

The pilot scale $H_2S$ scrubbing system was set up with the combination of liquid bed and the column considering the

optimized conditions from lab-scale experiments to evaluate the system's performance for a 1cu.m digester. The liquid bed setup was set up in a 35 L HDPE barrel with a provision for the inlet and outlet on the top. The inlet pipe was extended in an "L" shape inside the barrel at the bottom, and 2 mm perforations were provided for uniform diffusion of the inflowing gas. The outlet is provided as represented in Fig. 2. The barrel was filled with 30 L of *Thiobacillus* culture. The column setup was fabricated using PVC pipe with an 11 cm diameter and height of 1.5 m with 1 m working volume and 0.5 m head space. The column was filled with equal volumes of PS and CP. Before the experiment began, the column was added with 1 L of the culture. The biogas inflow was given at the rate of 1.5 cu.m.$hr^{-1}$ with a provision to regulate the flow rate. The setup was connected in series such that the outlet of the liquid bed was connected to the inlet of the column. The outlet at the top of the column was connected to the biogas meter to record the $H_2S$ concentrations. Fig. 2 shows the flow diagram representing the setup and the real-time picture of the setup.

## RESULTS AND DISCUSSION

### Effect of Different Parameters on Absorption in Liquid Bed Studies

The effect of time on the absorption represents the capacity of the LM to the extent to which the particular molecule will be absorbed. Fig. 3 [a] represents the effect of time on absorption. As time increases, it was observed that the absorption of the $H_2S$ gradually increases, attaining saturation. In the initial 8 min, the $H_2S$ concentration reached 287 ppm from 147 ppm. Further, from 287 ppm, the saturation concentration, i.e., 467 ppm, was reached at 75 min. The total time observed for the culture to saturate was 75 min keeping other parameters such as flow rate, amount of culture, and initial concentrations constant at 1 L.$min^{-1}$, 250 mL, and 467 ppm, respectively.

The study on the amount of culture was found to be a significant parameter affecting the process of absorption (Fig. 3 [b]). Three different volumes were considered for the study, and it was evident that the highest volume was more efficient than the rest. For the experiment with 500 mL LM, it was observed that in the first 20 min, the concentration of $H_2S$ was reduced to 34 ppm from 467 ppm, and in the 25$^{th}$ min, the concentration reached 134 ppm. The concentration gradually increased with time till 60$^{th}$ min and was observed to attain saturation. A similar trend was seen with 100 and 200 mL of LM. For 100 mL, the saturation was achieved at the 5$^{th}$ and 200 mL at the 45$^{th}$ min, respectively.

When the flow rate was studied (Fig. 3 [c]), the highest flow rate, 1.2 L.$min^{-1}$, was the least effective, while the lowest flow rate showed better results. The saturation for 1.2 L.$min^{-1}$ was reached in no time (<1 min) whereas, at

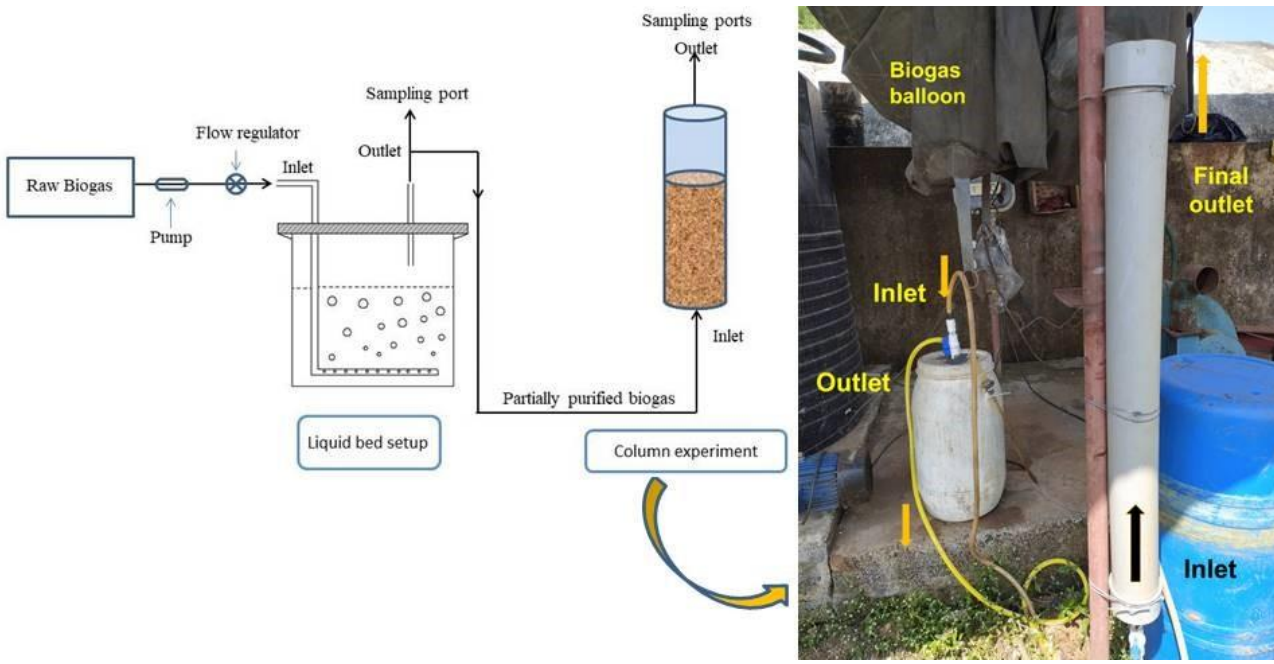


Fig. 2: Set up illustrating the combination of liquid bed and continuous column at pilot scale.

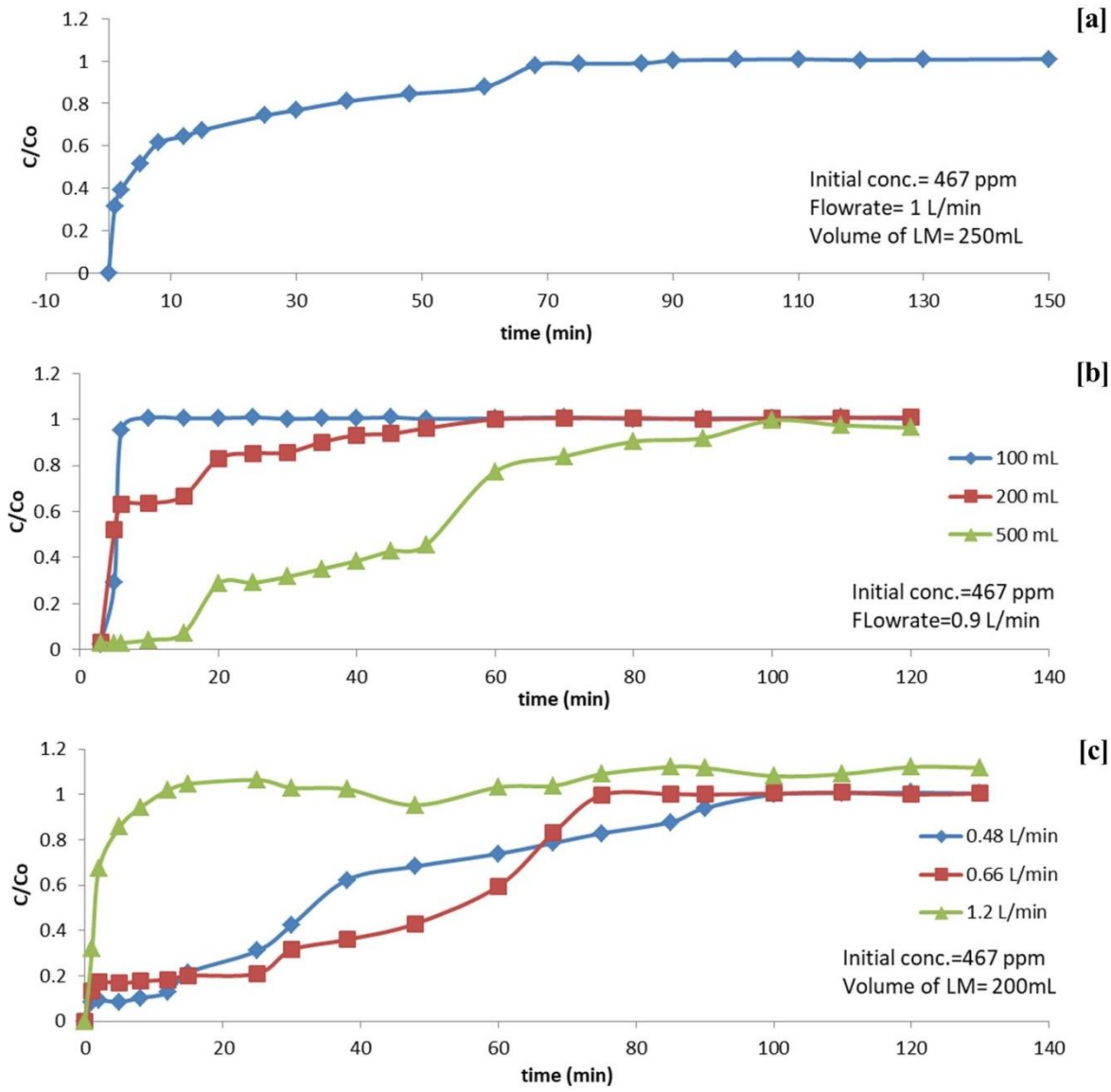


Fig. 3: Graphical representation of plot between time and C/Co for [a] time, [b] volume of culture, and [c] flow rate for liquid bed experiments.

0.66 L.min$^{-1}$ flow rate, the saturation reached at 75$^{th}$ min with an increase in $H_2S$ concentration from 78 ppm to >467 ppm. The best flow rate found to be 0.48 L.min$^{-1}$ showed a maximum $H_2S$ removal until the 12$^{th}$ min with 98 ppm and a linear increase until the 38$^{th}$ min to 291 ppm, followed by a gradual increase to achieve saturation at the 90$^{th}$ min.

The absorption of $H_2S$ in the LM can be studied with reference to the oxidation rate of sulfur. The gas retention time (GRT) and loading rate were calculated before calculating the biological oxidation rate. The formulae for the above parameters are as follows,

$$GRT = \frac{V}{Q} \quad ...(1)$$

Where GRT is the gas retention time (min), V is the volume of absorbers (L), and Q is the gas flow rate (L.min$^{-1}$).

$$\text{H2S loading} = \frac{(QXC)}{V} \quad ...(2)$$

Where $H_2S$ loading is in g.m$^{-3}$.h$^{-1}$, and C is the inlet concentration (g-S/L).

$$\text{Oxidation rate} = \frac{(Co-Ci).Q}{V} \quad ...(3)$$

Where Co is the $H_2S$ concentration of the medium leaving the LM ($g.L^{-1}$), and Ci is the $H_2S$ concentration of the medium flow into the LM ($g.L^{-1}$) (Lin et al. 2013).

As anticipated, the GRT of the three different volumes of culture increased as the volume increased. The highest volume was chosen, i.e., 500 mL showed the highest GRT as 0.555 min. Seemingly the $H_2S$ loading rate showed a maximum for the lowest volume of 100 mL as 4.20 $g.m^{-3}.h^{-1}$, and a decrease was observed as the volume increased. Similarly, for other parameters, flow rate, the GRT, and $H_2S$ loading rates were found maximum for the highest flow rate set (i.e., 1.2 $L.min^{-1}$) as 0.833 min and 5.60 $g.m^{-3}.h^{-1}$, respectively, concluding that the parameters were well within the experiment. All the other values for every parameter are listed in Table 3. Fig. 4 and Table 3 represent the variation in the oxidization rate at every step. As can be observed from the Fig. 4 [b], the lowest volume of culture showed the highest oxidation rate occurring but for a substantially minimal time. However, as the volume increases, the time taken for the oxidation also increases but at a lower oxidation rate when compared to 100 mL volume.

Similarly, for different flow rates, 0.48, 0.66, and 1.2 $L.min^{-1}$, the highest oxidation rates recorded were 70.5, 35.01, and 13.6 $ppm.sec^{-1}$, respectively. After several minutes of operation, the oxidation rate expressed a negative value, showing that sulfur oxidation has stopped and no further conversion is possible. The average oxidation rate was calculated considering all the positive values of oxidation rates, which were found to be in decreasing order and are reported in Table 3 and can be observed in Fig. 4.

## Effect of Parameters on Adsorption in Column Experiments

The column studies allowed us to investigate more parameters than the liquid bed study with five different parameters: time, bed height, culture volume, flow rate, and filling ratio. From the literature, it was found that the increase in dissolved oxygen (DO) decreases the elemental sulfur (Doungprasopsuk & Suwanvitaya 2017). However, in the current study, DO was not considered, as the raw biogas had no DO present. The adsorption is a time-dependent process. Hence, the other parameters were fixed, and the time parameter was studied. Fig. 5 [a] represents the effect of time on the adsorption of $H_2S$. With the initial concentration of 467 ppm and flow rate of 0.9 $L.min^{-1}$, the adsorption was achieved up to 25%. At the 90$^{th}$ min, saturation occurs, and no changes were observed between the inlet and outlet concentration of $H_2S$.

Furthermore, the bed height showed a significant difference in the result. All three heights selected showed

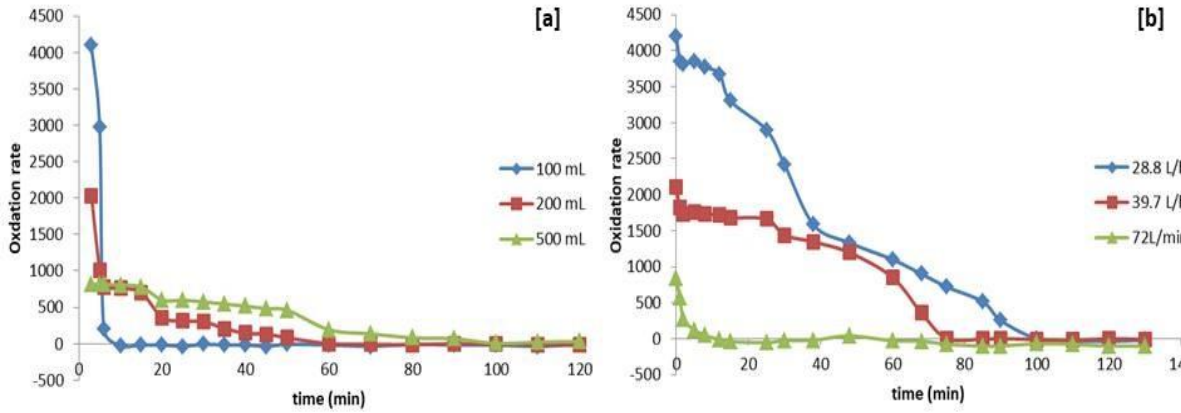


Fig. 4: Graphical representation of oxidation rate for [a] volume of LM and [b] flow rate for liquid bed experiments.

Table 3: The parameters related to absorption of $H_2S$.

| | | GRT (min) | $H_2S$ loading [$g.m^{-3}.h^{-1}$] | Max. oxidation rate [$ppm.min^{-1}$] | Avg. oxidation rate [$ppm.min^{-1}$] |
|---|---|---|---|---|---|
| Volume | 100 mL | 0.111 | 4.203 | 4095 | 2421 |
| | 200 mL | 0.222 | 2.101 | 2034 | 568.1 |
| | 500 mL | 0.555 | 0.840 | 817.2 | 438.6 |
| Flow rate | 0.48 $L.min^{-1}$ | 0.208 | 2.24 | 4203 | 2386.1 |
| | 0.66 $L.min^{-1}$ | 0.151 | 3.08 | 2101.5 | 1385.3 |
| | 1.2 $L.min^{-1}$ | 0.833 | 5.60 | 840.6 | 370.8 |

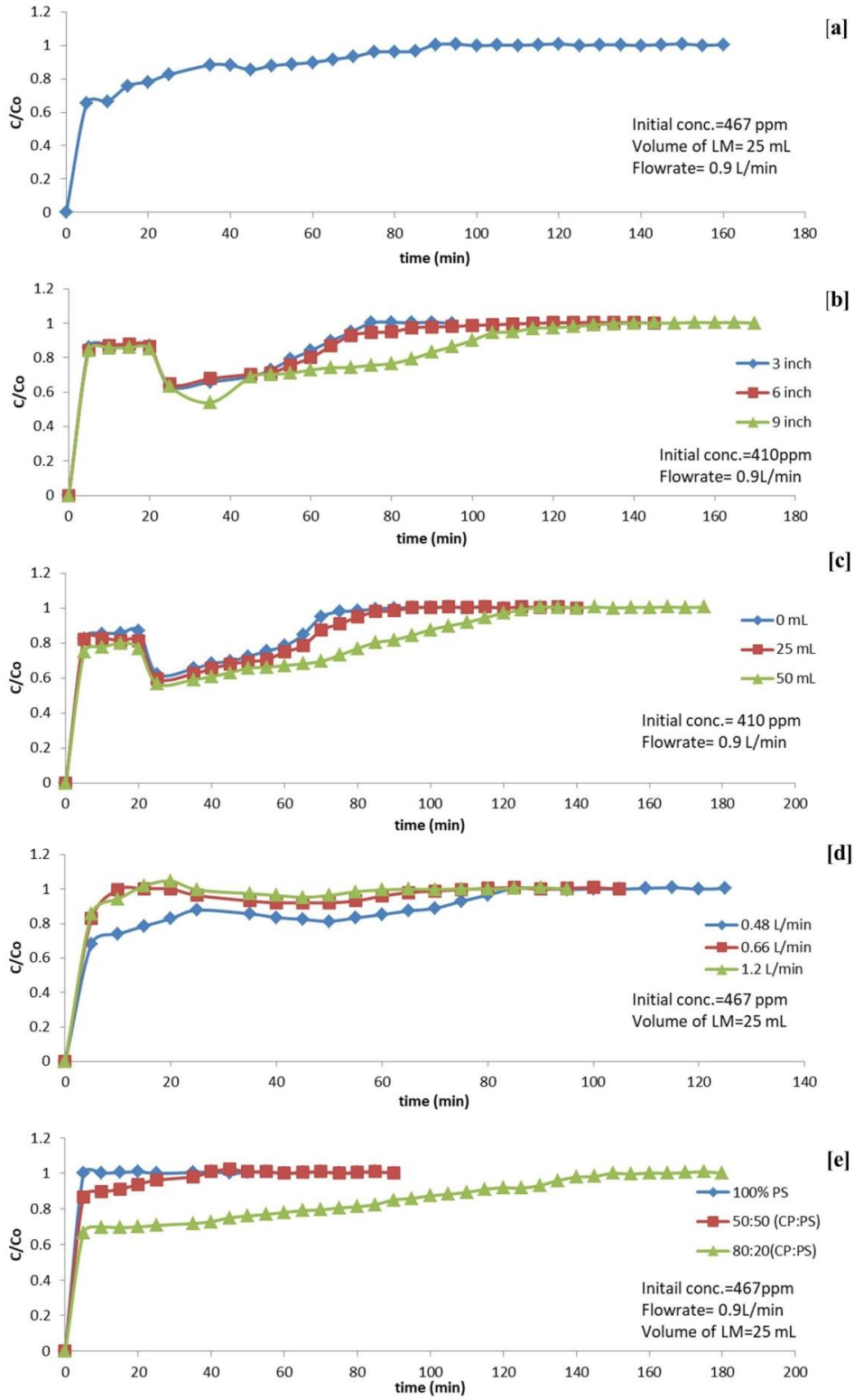


Fig. 5: Graphical representation of plot between time and normalized concentration for [a] time, [b] bed height, [c] volume of culture, [d] flow rate, and [e] filling ratio of the column for continuous column experiments.

around 20% adsorption for the first 20 min. However, this trend changed at the 26$^{th}$ min, and a sudden drop in efficiency was seen. This peculiar behavior can be inferred as single-layer adsorption taking place as biogas enters the column and the efficiency reduces. As the biogas adsorption enters the multi-layer regime, the performance increases; hence a steep decrease in the concentration can be seen. Similar behavior was seen for all the parameters studied. The highest bed height of 9 inches showed better results than the other two, with a saturation time of 110 min of continuous operation. The three and 6-inch bed height columns saturated at 70$^{th}$ and 90$^{th}$ min, respectively.

The column with CP and PS without LM showed adsorption of about 20% at the initial time of operation. The 50 mL LM selected showed similar results as the controls initially. The trend changed at 30 min as the peak gradually increased towards saturation than the control. The flow rate affected the column performance as expected. The higher flow rate, 1.2 mL.min$^{-1}$, showed rapid saturation at 15 min, whereas the lowest selected flow rate, 0.48 mL.min$^{-1}$, showed complete saturation at 80 min with 25 mL of culture and an initial $H_2S$ concentration of 467 ppm.

The filling ratio of the column is essential when two or more adsorbents are used. The combination of CP and PS was studied as CP acts as an adsorbent along with LM, and the PS provides porosity in the column. The CP was used in many of these studies as an adsorbent to remove ammonia from the waste stream (Baquerizo et al. 2009). It has been used to remove various types of dyes from wastewater (Chong & Tam 2020).

The 100% CP was used to study the efficiency of the column toward the adsorption of $H_2S$. However, it was found not feasible as the addition of LM increased the moisture in the system, and the goo-like texture did not allow the air/biogas to pass through the column due to decreased medium porosity (Guo et al. 2007). Hence, an optimized ratio of these two will be necessary for large-scale implementation. The first column was selected with only PS, which reported no adsorption and allowed the biogas to pass through and reach the saturation levels at the first minute. The second column, selected with a 50:50 ratio of CP and PS, showed better results than the previous column. The third column, selected with an 80:20 ratio of CP and PS, showed the best results in removing the $H_2S$ from biogas. However, it had the disadvantage of not allowing the gas to pass through the column easily. The column output was significantly less, and most of the biogas either leaked due to back pressure or could not enter the column. Hence, this setup and the first column with 100% PS were forsaken. The literature suggested that the presence of higher concentrations of $H_2S$ (>500 ppm) in the inlet might lead to a decrease in a breakpoint, as it was also encountered in the present study (Georgiadis et al. 2021).

As this study mainly focused on the enrichment of biogas, the concentration of $CH_4$ is important in the further advancement of the experiments. The studies involving the removal of $H_2S$ might also affect the $CH_4$ concentration adversely. In these studies, the concentration of $CH_4$ and $CO_2$, along with $H_2S$, was recorded. Table 4 represents the amount of $CH_4$ and $CO_2$ at different optimized and selected conditions for the study. From the raw biogas, the reduction of $CH_4$ was assessed to be around 20%. With this representation of each condition set, it can be summarized that the $CH_4$ loss is minimal when the reduction of $H_2S$ is about 70% on average in the absorption study. From the literature, it was found that a $CO_2$ concentration of more than 200 ppm affects the $H_2S$ removal through the column (Georgiadis et al. 2021). In the present study, the concentration of $CO_2$ was around 25 ppm. $CO_2$ is a recalcitrant gas, which reduces the calorific value and density of the biogas (Aita et al. 2016). In the column studies, the $H_2S$ removal was found to be around 25%, and the $CH_4$ loss was around 22%. At the saturation point of $H_2S$, minimal removal of $CH_4$ of around 5% was noted, and most of the saturation levels showed no removal of $CH_4$. The variations in $CH_4$ are believed to be not from the adsorption through column constituents or due to the microbial culture. The study by Aita et al. (2016) and Montebello et al. (2013) state that $CH_4$ has a lower solubility in the liquid phase. Other literature by Salehi and Chaiprapat (2019) reveals that the methanogens present can take up $CH_4$. However, there are high chances of variations in pH which do not allow methanogens to proliferate (Aita et al. 2016).

Iron filings or iron oxide are also being used for $H_2S$ scrubbing. When hydrogen sulfide reacts with iron oxide, it produces iron sulfide, an iron sponge (Andriani et al. 2020). However, the disposal of this is the main issue when it comes to the use of iron sponges. The study conducted by Bagreev et al. (2000) used activated carbon which also oxidizes $H_2S$ to elemental sulfur (Bagreev et al. 2000). These procedures either increases the cost of the process or may become difficult to dispose of or regenerate the used column constituents after saturation.

## Adsorption Kinetics, Isotherms, and Models for Continuous Column Studies

The validation of any adsorption process can be done by the study of adsorption kinetics and adsorption isotherms. Kinetics studies the relationship between the retention time of the adsorbent in any media interface and the ion removal rate (Guo et al. 2007). Kinetics is an important validation step to determine the adsorption rate (Habeeb et al. 2016).

Table 4: Comparison of $CH_4$ and $CO_2$ removal in pilot scale study along with $H_2S$.

| | Raw biogas conc. | | | Intermediate conc. | | | Saturation conc. at $n^{th}$ min | | |
|---|---|---|---|---|---|---|---|---|---|
| | $CH_4$ | $CO_2$ | $H_2S$ | $CH_4$ | $CO_2$ | $H_2S$ | $CH_4$ | $CO_2$ | $H_2S$ |
| Absorption studies | | | | | | | | | |
| Amount of culture | 53.5 | 25.6 | 467 | 42.2 | 22.3 | 137 | 48.6 | 23.7 | 469 |
| Flow rate | 53.5 | 25.6 | 467 | 48 | 13.8 | 150 | 48.1 | 23 | 470 |
| Adsorption studies | | | | | | | | | |
| Time | 55.9 | 26.9 | 410 | 43.6 | 24.3 | 346 | 53.9 | 25.7 | 411 |
| Bed height | 55.9 | 26.9 | 410 | 43.4 | 26.2 | 307 | 54.3 | 25.3 | 412 |
| Amount of culture | 55.9 | 26.9 | 410 | 45.3 | 26.5 | 304 | 53.6 | 25.4 | 412 |
| Flow rate | 53.5 | 25.6 | 467 | 42.5 | 22.1 | 298 | 52.6 | 25.8 | 469 |
| Filling ratio | 53.5 | 25.6 | 467 | 49.5 | 22.5 | 295 | 52.4 | 25.2 | 470 |

Hence, three requisite models were considered for the study: pseudo-first order, pseudo-second order, and Elovich model. The adsorption isotherm is a transit for understanding the relationship among the active sites of absorbent and the adsorbate at constant temperature (Guo et al. 2007). Off the adsorption isotherms, Langmuir isotherm and Freundlich isotherms were studied (Ayiania et al. 2019, Shah et al. 2017). The following two formulas were used to calculate the adsorbents' adsorption capacity and efficiency.

$$R\ (\%) = \left(\frac{Co-Ce}{Co}\right) \times 100 \quad \ldots(4)$$

$$qe = \left(\frac{Co-Ce}{m}\right) \times V \quad \ldots(5)$$

Where Co and Ce are the initial and equilibrium concentrations of $H_2S$, respectively; V is the volume of the solution (L); m is the amount of adsorbent (g); 'qe' is the absorption capacity ($mL.g^{-1}$) and R% is the adsorption percentage.

The 'qe' determines the extent of the occurrence of adsorption. The logarithmic curve between the time and 'qe' represents the adsorption capacity of the individual adsorbent. Fig. 6 shows a plot between the same and the logarithmic curve observed until the $60^{th}$ min. Later the decrement path was observed. The adsorption kinetics study evaluates the rate-controlling steps involved in the process (Georgiadis et al. 2021). The pseudo-second-order

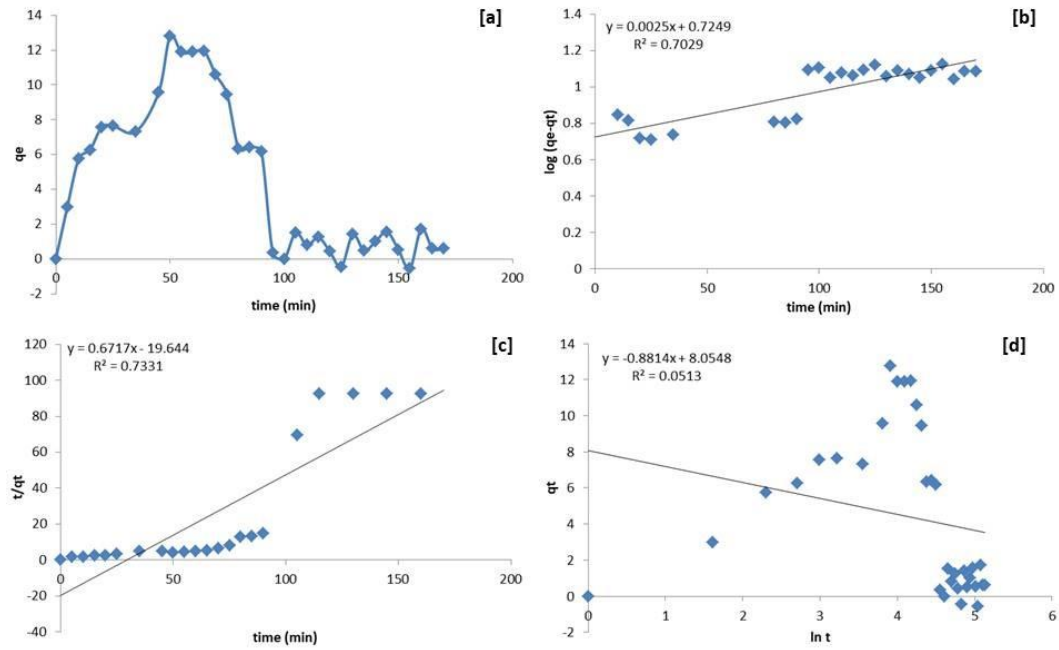


Fig. 6: Plots depicting [a] adsorption capacity of adsorbent, [b] pseudo-first-order, [c] pseudo-second-order, and [d] Elovich, model.

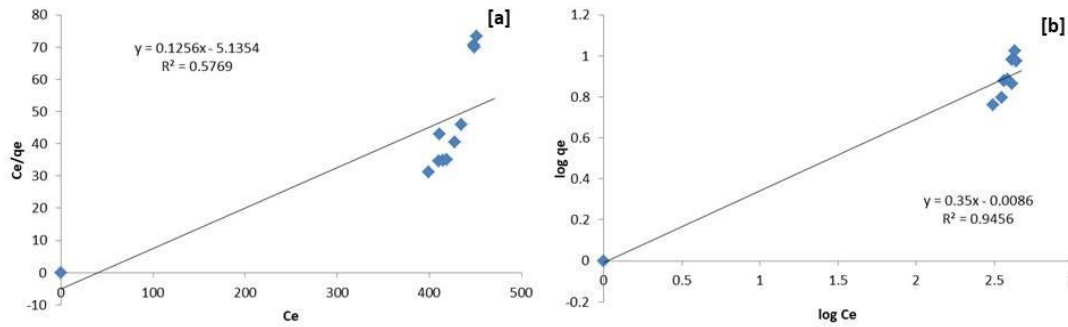


Fig. 7: Plots depicting [a] Langmuir and [b] Freundlich isotherm.

model was the best-fitted kinetic model for the present study, with $R^2 = 0.7331$. The pseudo-second-order kinetics provides the best correlation for the experimental data, and the adsorption mechanism is a chemically rate-controlling step in the adsorption. The other models, i.e., pseudo-first-order and Elovich models, showed $R^2 = 0.7029$ and 0.0513, respectively. This resulted in the limelight on the non-fitting models (Fig. 6). The Elovich model brings an understanding of whether the reaction is chemical in nature or not.

Although this model did not fit the current study, the other isotherm studies proved the process. When the adsorption isotherms were studied, it was found that the process followed the Freundlich model with $R^2 = 0.9456$. Correspondingly, it made us understand that adsorption occurs on heterogonous surfaces (multilayer adsorption) (Bagreev et al. 2005). The 'n' value from the linear equation is important because it described the quality of the adsorption taking place and was found to be 0.35 for the present study. The $R^2$ value for Langmuir isotherm was 0.5769, which did not follow the adsorption conditions. Fig. 7 represents linear equations for each model studied, and Table 5 shows the parameters of the studied models.

In the present study, four continuous column-based models were studied. Every model describes conditions for fulfilling the adsorption process being valid. The Thomas model gives an understanding of the dynamics of the process (Sunzini et al. 2020). The plot for the Thomas model is presented as Fig. 8. The $R^2$ and kth values were found to be 0.7889 and -0.7819. Other models, such as the Yoon-Nelson model and BDST, showed $R^2$ as 0.9301 and 0.9911, where the BDST model was

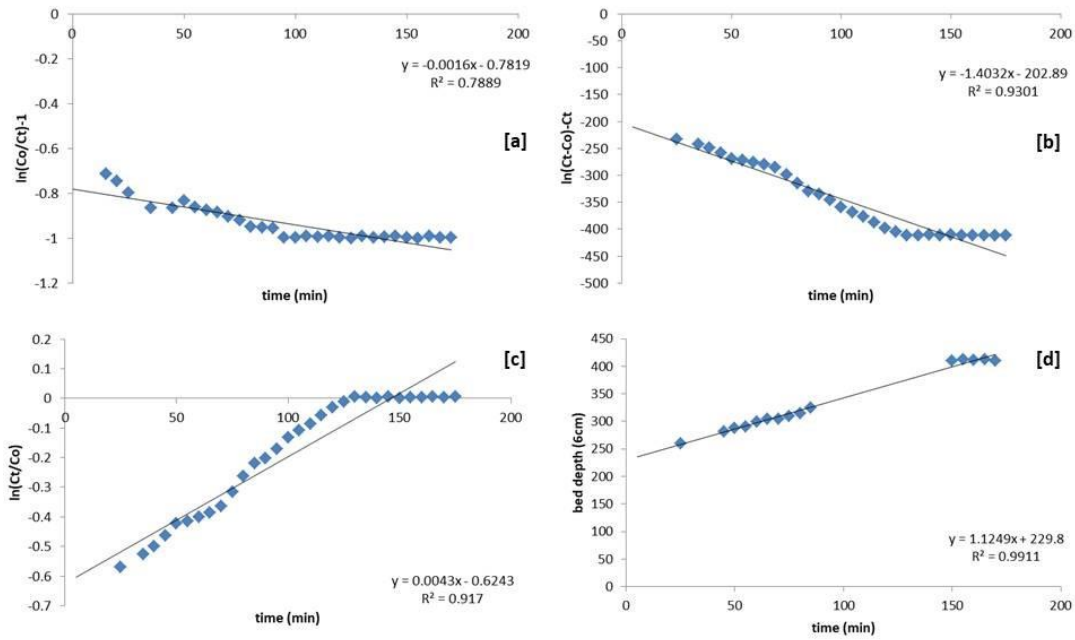


Fig. 8: Plots depicting [a] Thomas model, [b] Yoon-Nelson model, [c] Adams–Bohart model, and [d] BDST model.

Table 5: Parameters of kinetics and isotherms for adsorption.

| Models | Parameters | | Models | Parameters | |
|---|---|---|---|---|---|
| Adsorption kinetics | | | Continuous column experiments | | |
| Pseudo first order | $q_e$ | 0.7249 | Thomas model | $k_{th}$ | -0.7819 |
| | $k_1$ | 0.0025 | | $R^2$ | 0.7889 |
| | $R^2$ | 0.7029 | Yoon-Nelson model | $k_{YN}$ | -1.403 |
| Pseudo second order | $q_e$ | -19.64 | | $\tau$ | -202.89 |
| | $k_1$ | 0.6717 | | $R^2$ | 0.9301 |
| | $R^2$ | 0.7331 | Adams-Bohart model | $k_{AB}$ | 0.0043 |
| Elovich model | $\alpha$ | 8.054 | | $N_o$ | -0.6243 |
| | $\beta$ | -0.8814 | | $R^2$ | 0.917 |
| | $R^2$ | 0.0513 | BDST | $N_o$ | 1.12 |
| Adsorption isotherms | | | | $k_a$ | 229.8 |
| Langmuir isotherm | $q_m$ | 0.125 | | $R^2$ | 0.9911 |
| | b | - 5.13 | | | |
| | $R^2$ | 0.5739 | | | |
| Freundlich isotherm | n | 0.35 | | | |
| | $k_f$ | -0.0086 | | | |
| | $R^2$ | 0.9456 | | | |

the best fit. The equation constants for each model were $k_{YN}$ = -1.403, $k_{AB}$ = 0.0043, and $k_a$ = 229.8, respectively.

The Yoon-Nelson model explains the 50% of the time required for the adsorbate breakthrough (Zulkefli et al. 2017). The rationale of the BDST model is that equilibrium is not immediate in the bed. Therefore, the rate of the sorption process is directly proportional to the fraction of sorption capacity remaining on the media (Aslam et al. 2019). All the parameters associated with the kinetic and isotherm study are presented in Table 5.

## Performance of Pilot-scale $H_2S$ Scrubbing System

The optimized conditions from the lab-scale experiments were selected to operate the setup at a larger scale. At a large scale, liquid bed and column setup were combined with increasing the system's overall efficiency. The optimized conditions, such as a filling ratio of 50% of CP and 50% of PS, were uptaken. The column height was 1.5 m with 1 m of the working volume and 0.5 m headspace. The flow rate was fixed as 0.9 $m^3.h^{-1}$, and liquid beds were prepared in a 35 L HDPE tank with 30 L of LM with *Thiobacillus*

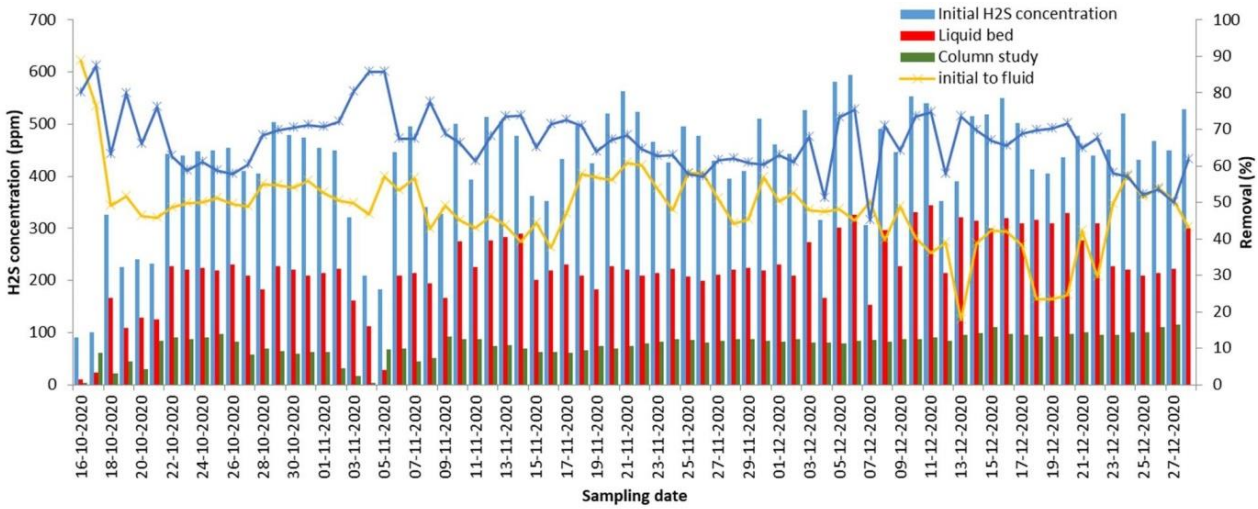


Fig. 9: Graphical illustration of removal of $H_2S$ from biogas at every stage for the pilot scale setup.

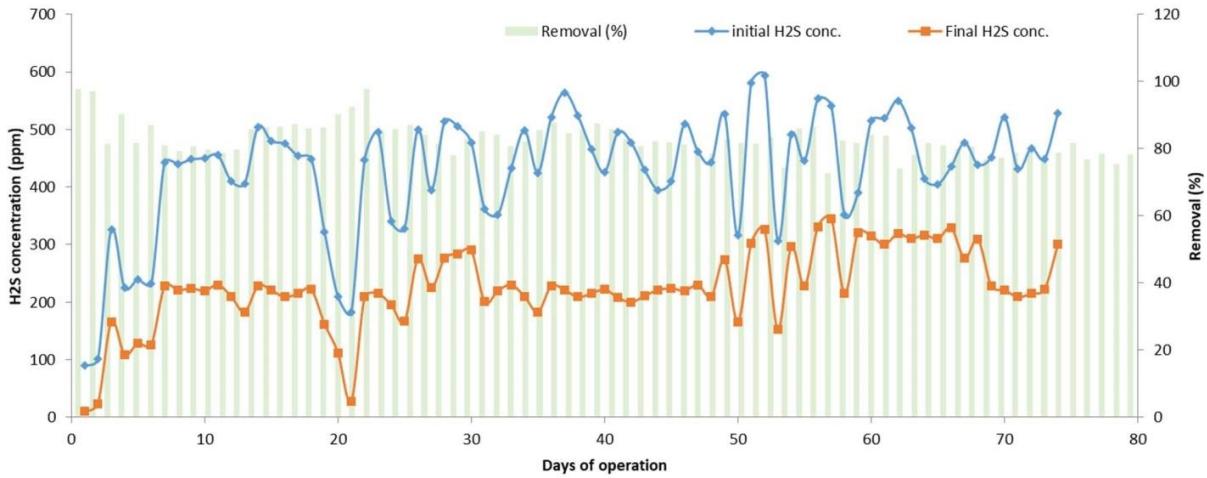


Fig. 10: Graphical representation of overall removal of $H_2S$ from biogas and efficiency at pilot scale setup.

sp. culture added. The outlet concentration from the liquid bed and the column were recorded periodically along with the inlet concentrations. Every day around 1.5 $m^3$ of biogas was passed through the setup. The column and the liquid bed did not attain complete saturation even after 2 months of continuous operation. A small decrease in efficiency was observed after purging 1.5 $m^3$ of raw biogas. However, this did not affect the next day's performance which showed better efficiency in removing $H_2S$. The addition of LM was done when the moisture in the column decreased, and this was done 4 times during the entire operation. The liquid bed was never refilled or replenished with the new culture.

Fig. 9 shows the variations in the concentrations of $H_2S$. As can be observed from the graphical representation, an average of 50% removal of $H_2S$ was seen with the liquid bed. 20% more removal was possible by introducing a column in series with the liquid bed. An average of 70-75% of $H_2S$ removal was recorded. The study conducted by Pantoja et al. (2010) encountered above 99% removal of $H_2S$ with CP (Pantoja et al. 2010). This was possible due to the particle size of CP. As the size of the particles is reduced, higher adsorption is achieved (Cherosky 2012). The average inlet concentration was 500 ppm of $H_2S$ and 65% $CH_4$. At the end of the combined treatment, the $H_2S$ concentration was less than 50 ppm, with 55-60% $CH_4$ in the biogas. Fig. 10 explains the overall treatment of the system from initial to final concentration. Another study by Habeeb et al. (2016) removed liquid sulfide from wastewater using CP. It was evident that the use of CP adsorbed high concentrations of $H_2S$. In addition, the LM boosted the efficiency to a higher level.

## CONCLUSIONS

The study began with a focus on enriching the biogas with $CH_4$ and evaluating its relevance for commercial application. The in-depth study of the adsorption and absorption of $H_2S$ helped to set up the pilot-scale treatment system. By evaluating the laboratory scale study, it was found that the $H_2S$ concentration could be minimized using the combination of LM containing *Thiobacillus sp*. culture with the column containing CP and PS with the LM. These setups were studied individually to know the adsorption, absorption, and microbial conversion. The evaluation study aided in understanding the extent of adsorption in the system. The treatment becomes effective when both the systems are combined, i.e., passing the $H_2S$-rich biogas through the LM containing *Thiobacillus* sp. culture than through the column. The present study showed that passing biogas through the LM with culture was more efficient than using a column. Since the efficiency needed to be maximized, combining the two was necessary. The combined pilot scale setup successfully reduced the $H_2S$ concentration to 75% with only 5-8% of $CH_4$ loss, which can be undervalued as the reduction in the $H_2S$ concentration was observed from 500 ppm to less than 50 ppm. The experimental setup successfully ran for over 8 weeks without replenishing the LM with fresh culture. However, the column was added with fresh culture to balance the moisture. The setup was successful in both laboratory and pilot scales and treated 1.5 $m^3$ of raw biogas daily.

## ACKNOWLEDGMENTS

The authors thank the BITS Pilani K.K. Birla Goa Campus for providing facilities to conduct the experiments and construct the pilot scale reactors at the Sewage treatment plant (STP).

## REFERENCES


Aita, B.C., Mayer, F.D., Muratt, D.T., Brondani, M., Pujol, S.B., Denardi, L.B. and Da Silveira, D.D. 2016. Biofiltration of H2S-rich biogas using Acidithiobacillus thiooxidans. Clean Technol. Environ. Policy, 18(3): 689-703.

Andriani, D., Rajani, A., Santosa, A., Saepudin, A., Wresta, A. and Atmaja, T. 2020. A review on biogas purification through hydrogen sulphide removal. IOP Conf, Ser. Earth Environ. Sci., 16: 545-563.

Aslam, Z., Hussein, I.A., Shawabkeh, R.A., Parvez, M.A., Ahmad, W. and Ihsanullah, M. 2019. Adsorption kinetics and modeling of $H_2S$ by treated waste oil fly ash. J. Air Waste Manag. Assoc., 69(2): 246-257.

Ayiania, M., Carbajal-Gamarra, F.M., Garcia-Perez, T., Frear, C., Suliman, W. and Garcia-Perez, M.J.B. 2019. Production and characterization of $H_2S$ and PO43– carbonaceous adsorbents from anaerobic digested fibers. Biomass Bioenergy, 120: 339-349.

Bagreev, A., Rahman, H. and Bandosz, T. 2000. Study of $H_2S$ adsorption and water regeneration of spent coconut-based activated carbon. Environ. Sci. Technol., 34(21): 4587-4592.

Bagreev, A.A., Kuang, W. and Bandosz, T.J. 2005. Predictions of $H_2S$ breakthrough capacity of activated carbons at low concentrations of hydrogen sulfide. Adsorption, 11(1): 461-466.

Baquerizo, G., Maestre, J.P., Machado, V.C., Gamisans, X. and Gabriel, D. 2009. Long-term ammonia removal in a coconut fiber-packed biofilter: Analysis of N fractionation and reactor performance under steady-state and transient conditions. Water Res., 43(8): 2293-2301.

Cherosky, P.B. 2012. Anaerobic Digestion of Yard Waste and Biogas Purification by Removal of Hydrogen Sulfide. The Ohio State University, Ohio.

Chong, M.Y. and Tam, Y.J. 2020. Bioremediation of dyes using coconut parts via adsorption: A review. SN Appl. Sci., 2(2): 1-16.

de Oliveira, L.H., Meneguin, J.G., Pereira, M.V., da Silva, E.A., Grava, W.M., do Nascimento, J.F. and Arroyo, P.A. 2019. H2S adsorption on NaY zeolite. Micropor. Mesopor. Mater., 284: 247-257.

De Silvaa, J.A., Karunaratnea, A. and Sumanasinghea, V. 2019. Wastewater treatment using attached growth microbial biofilms on coconut fiber: A short review. J. Agric. Value Add., 2(1): 61-70.

Díaz, I., Pérez, S., Ferrero, E. and Fdz-Polanco, M. 2011. Effect of oxygen dosing point and mixing on the microaerobic removal of hydrogen sulphide in sludge digesters. Bioresour. Technol., 102(4): 3768-3775.

Doungprasopsuk, W. and Suwanvitaya, P. 2017. Effect of oxygen on sulfur products from $H_2S$ removal by Thiobacillus in a biotrickling filter column. Eng. Appl. Sci. Res., 44(4): 214-221.

Dumont, E. (2015). H2S removal from biogas using bioreactors: a review. Int. J. Energy Environ., 6(5): 479-498.

Fischer, M.E. 2010. Biogas Purification: $H_2S$ removal Using Biofiltration. The University of Waterloo,

Georgiadis, A.G., Charisiou, N.D., Gaber, S., Polychronopoulou, K., Yentekakis, I.V. and Goula, M.A. 2021. Adsorption of hydrogen sulfide at low temperatures using an industrial molecular sieve: An experimental and theoretical study. Acs Omega, 6(23): 14774-14787.

Guo, J., Luo, Y., Lua, A.C., Chi, R.A., Chen, Y.l., Bao, X.T. and Xiang, S.X. 2007. Adsorption of hydrogen sulphide ($H_2S$) by activated carbons derived from oil-palm shell. Carbon, 45(2): 330-336.

Habeeb, O., Ramesh, K., Ali, G.A., Yunus, R., Thanusha, T. and Olalere, O. 2016. Modeling and optimization for $H_2S$ adsorption from wastewater using coconut shell-based activated carbon. Aust. J. Basic Appl. Sci., 10(17): 136-147.

Ho, K.L., Lin, W.C., Chung, Y.C., Chen, Y.P. and Tseng, C.P. 2013. Elimination of high concentration hydrogen sulfide and biogas purification by chemical–biological process. Chemosphere, 92(10): 1396-1401.

Jensen, A.B. and Webb, C. 1995. Treatment of $H_2S$-containing gases: A review of microbiological alternatives. Enzy. Microb. Technol., 17(1): 2-10.

Kulkarni, M. and Ghanegaonkar, P. 2019. Hydrogen sulfide removal from biogas using chemical absorption technique in packed column reactors. Glob. J. Environ. Sci. Manag., 5(2): 155-166.

Kumari, R. and Dey, S. 2019. A breakthrough column study for removal of malachite green using coco-peat. Int. J. Phytoremed., 21(12): 1263-1271.

Lin, W.C., Chen, Y.P. and Tseng, C.P. 2013. Pilot-scale chemical–biological system for efficient $H_2S$ removal from biogas. Bioresour. Technol., 135: 283-291.

Montebello, A.M., Bezerra, T., Rovira, R., Rago, L., Lafuente, J., Gamisans, X. and Gabriel, D. 2013. Operational aspects, pH transition and microbial shifts of an $H_2S$ desulfurizing biotrickling filter with random packing material. Chemosphere, 93(11): 2675-2682.

Monteleone, G., De Francesco, M., Galli, S., Marchetti, M. and Naticchioni, V. 2011. Deep $H_2S$ removal from biogas for molten carbonate fuel cell (MCFC) systems. Chem. Eng., 173(2): 407-414.

Pantoja, J.L.R., Sader, L.T., Damianovic, M.H.R.Z., Foresti, E. and Silva, E.L. 2010. Performance evaluation of packing materials in the removal of hydrogen sulphide in gas-phase biofilters: polyurethane foam, sugarcane bagasse, and coconut fibre. Chem. Eng., 158(3): 441-450.

Pokorna, D. and Zabranska, J. 2015. Sulfur-oxidizing bacteria in environmental technology. Biotechnol. Adv., 33(6): 1246-1259.

Ramírez-Aldaba, H., Valles, O.P., Vazquez-Arenas, J., Rojas-Contreras, J.A., Valdez-Pérez, D., Ruiz-Baca, E. and Lara, R.H. 2016. Chemical and surface analysis during the evolution of arsenopyrite oxidation by Acidithiobacillus thiooxidans in the presence and absence of supplementary arsenic. Sci. Total Environ., 566: 1106-1119.

Salehi, R. and Chaiprapat, S. 2019. Single-/triple-stage biotrickling filter treating an $H_2S$-rich biogas stream: statistical analysis of the effect of empty bed retention time and liquid recirculation velocity. J. Air Waste Manag. Assoc., 69(12): 1429-1437.

Sethupathi, S., Zhang, M., Rajapaksha, A.U., Lee, S.R., Mohamad Nor, N., Mohamed, A.R. and Ok, Y.S. 2017. Biochars as potential adsorbers of $CH_4$, $CO_2$, and $H_2S$. Sustainability, 9(1): 121.

Shah, M.S., Tsapatsis, M. and Siepmann, J.I. 2017. Hydrogen sulfide capture: From absorption in polar liquids to oxide, zeolite, and metal-organic framework adsorbents and membranes. Chem. Rev., 117(14): 9755-9803.

Sunzini, F., De Stefano, S., Chimenti, M.S. and Melino, S. 2020. Hydrogen sulfide as potential regulatory gasotransmitter in arthritic diseases. Int. J. Mol. Sci., 21(4): 1180.

Zhang, L., De Schryver, P., De Gusseme, B., De Muynck, W., Boon, N. and Verstraete, W. 2008. Chemical and biological technologies for hydrogen sulfide emission control in sewer systems: A review. Water Res., 42(1-2): 1-12.

Zhao, Q., Leonhardt, E., MacConnell, C., Frear, C. and Chen, S. 2010. Purification technologies for biogas generated by anaerobic digestion. Compr. Biometh., 24: 625.

Zhu, H.L., Papurello, D., Gandiglio, M., Lanzini, A., Akpinar, I., Shearing, P.R. and Zhang, Y.S. 2020. Study of $H_2S$ removal capability from simulated biogas by using waste-derived adsorbent materials. Processes, 8(9): 1030.

Zicari, S.M. 2003. Removal of hydrogen sulfide from biogas using cow-manure compost. Citeseer, 11: 22-36.

Zulkefli, N.N., Masdar, M.S., Isahak, W., Jahim, J., Majlan, E., Rejab, S. and Lye, C. 2017. Mathematical modeling and simulation on the adsorption of Hydrogen Sulfide ($H_2S$) gas. IOP Conf. Ser. Mater. Sci. Eng., 1603: 150411.